Published in final edited form as:
J Autoimmun. 2010 December ; 35(4): . doi:10.1016/j.jaut.2010.09.003.

CXCL10 promotes liver fibrosis by prevention of NK cell mediated hepatic stellate cell inactivation

Edith Hintermann[a], **Monika Bayer**[a], **Josef M. Pfeilschifter**[a], **Andrew D. Luster**[b], and **Urs Christen**[a,*]

[a] Pharmazentrum Frankfurt/ZAFES, Johann Wolfgang Goethe University, Frankfurt am Main, Germany

[b] Massachusetts General Hospital, Harvard Medical School, Charlestown, MA, USA

Abstract

Chemokines, such as CXCL10, promote hepatic inflammation in chronic or acute liver injury through recruitment of leukocytes to the liver parenchyma. The CXCL10 receptor CXCR3, which is expressed on a subset of leukocytes, plays an important part in Th1-dependent inflammatory responses. Here, we investigated the role of CXCL10 in chemically induced liver fibrosis. We used carbon tetrachloride (CCl_4) to trigger chronic liver damage in wildtype C57BL/6 and CXCL10-deficient mice. Fibrosis severity was assessed by Sirius Red staining and intrahepatic leukocyte subsets were investigated by immunohisto-chemistry. We have further analyzed hepatic stellate cell (HSC) distribution and activation and investigated the effect of CXCL10 on HSC motility and proliferation. In order to demonstrate a possible therapeutic intervention strategy, we have examined the anti-fibrotic potential of a neutralizing anti-CXCL10 antibody. Upon CCl_4 administration, CXCL10-deficient mice showed massively reduced liver fibrosis, when compared to wildtype mice. CXCL10-deficient mice had less B- and T lymphocyte and dendritic cell infiltrations within the liver and the number and activity of HSCs was reduced. In contrast, natural killer (NK) cells were more abundant in CXCL10-deficient mice and granzyme B expression was increased in areas with high numbers of NK cells. Further detailed analysis revealed that HSCs express CXCR3, respond to CXCL10 and secrete CXCL10 when stimulated with IFNγ. Blockade of CXCL10 with a neutralizing antibody exhibited a significant anti-fibrotic effect. Our data suggest that CXCL10 is a pro-fibrotic factor, which participates in a crosstalk between hepatocytes, HSCs and immune cells. NK cells seem to play an important role in controlling HSC activity and fibrosis. CXCL10 blockade may constitute a possible therapeutic intervention for hepatic fibrosis.

Keywords

Hepatic fibrosis; Inflammation; Cellular trafficking; Hepatitis; Chemokine

1. Introduction

Hepatic fibrosis is a scarring response common to most forms of chronic liver injury, which can be caused by pathogens (hepatitis viruses, *Leishmania donovani*, *Schistosoma mansoni*), alcohol abuse, chemical toxins, as a side effect of the metabolic syndrome (nonalcoholic

* Corresponding author. Pharmazentrum Frankfurt, Klinikum der Johann Wolfgang Goethe Universität, Theodor-Stern Kai 7, 60590 Frankfurt am Main, Germany. Tel.: +49 69 6301 83105; fax: +49 69 6301 7663. christen@med.uni-frankfurt.de (U. Christen)..

steatohepatitis, NASH) or due to autoimmune liver disorders, such as autoimmune hepatitis (AIH), primary biliary cirrhosis (PBC) or primary sclerosing cholangitis (PSC) [1–8]. Liver fibrosis is characterized by an accumulation of extracellular matrix (ECM) proteins and a change in the type of ECM from the normal basement membrane-like matrix to a matrix rich in fibrillar collagens. An abnormal ECM composition jeopardizes the continuation of differentiated functions of all resident liver cells and results in cirrhosis, portal hypertension and finally in liver failure [1–3,9]. At the cellular level, noxious agents damage hepatocytes, inducing the recruitment of inflammatory cells and the activation of Kupffer cells, resulting in the release of cytokines, chemokines and growth factors [6,10,11]. The primary target cell in this inflammatory milieu is the HSC, which transdifferentiates from a quiescent retinoid-storing mesenchymal cell to an activated myofibroblast that expresses α-smooth muscle actin (αSMA) and is mainly responsible for the accelerated production of ECM in fibrotic tissue [1,3,9–11]. However, HSCs themselves express a multitude of soluble factors and as antigen-presenting cells participate in a complex cellular crosstalk [6,10,12].

An important chemokine responsible for the recruitment and localization of inflammatory cells to sites of tissue damage or infection is CXCL10 (IP10, IFN-inducible protein 10) [13–19]. It is bound by CXCR3, a receptor shared with CXCL4 (PF4, platelet factor 4; a very weak ligand), CXCL9 (Mig, monokine induced by IFNγ) and CXCL11 (I-TAC, IFN-inducible T cell α-chemoattractant) [20], which is expressed on CD4 and CD8 T cells, NK cells, B cells and dendritic cells (DCs) [21–23]. Several studies suggest a role of CXCL10 in the development of intrahepatic inflammation and fibrosis. First, in chronic hepatitis B and C patients, expression of genes encoding CXCL10 and CXCR3 was upregulated and expression levels correlated with disease severity [24–27]. CXCL10 was secreted by hepatocytes in areas of lobular inflammation in close proximity to $CXCR3^+$ CD8 T cells [25,27]. Second, CXCL10 serum levels have been found to be increased in patients with AIH [26]. Third, in patients with PBC and their relatives, the plasma level of CXCL10 and the frequency of $CXCR3^+$ cells were upregulated [26,28]. Interestingly, CXCL10 expression was apparent in portal areas, where also $CXCR3^+$ cells, which were primarily CD4 T cells, were found [28].

In mice, bile duct ligation, Concanavalin A treatment and toxic injury by CCl_4, D-galactosamine or methylene dianiline led to an increase in CXCL10 mRNA synthesis [29,30]. CXCL10 induction was also observed after two-third hepatectomy, a procedure which is followed by as strong regenerative response. A direct mitogenic effect of CXCL10 on hepatocytes could not be demonstrated [30]. However, a human fibroblast cell line secreted the potent hepatic mitogen hepatocyte growth factor upon treatment with CXCL10 and mice injected with CXCL10 showed increased CXCR2 expression, a receptor known for its hepatoprotective effect [30–32]. These findings suggest an indirect stimulatory role of CXCL10 in liver regeneration. In contrast, Yoneyama et al. reported an inhibitory effect of CXCL10 on hepatocyte proliferation [33].

In this study, we sought to investigate the role of cytokines in liver fibrosis. Since concanavalin A or LPS induced liver damage depends on the activation of T cells or B cells/macrophages [34,35], we decided to use CCl_4-mediated liver injury in order to avoid activation of a specific subset of lymphocytes but to induce general hepatotoxicity. In an initial screening for inflammatory factors in CCl_4-triggered fibrosis, we detected a massive increase in CXCL10 expression. Thus, we used CXCL10-deficient ($CXCL10^{-/-}$) mice and observed that absence of CXCL10 results in a much milder form of fibrosis with reduced numbers of liver infiltrating B- and T lymphocytes, but increased NK cell presence, highlighting the pro-fibrotic role of CXCL10 in chemically induced liver injury.

2. Material and methods

2.1. Mice, CCl_4 administration and antibody treatment

CXCL10$^{-/-}$ mice are on a C57BL/6 background [16]. Wildtype C57BL/6 mice were purchased from Harlan Netherlands (Horst, Netherlands). Carbon tetrachloride (CCl_4) was from Sigma-Aldrich (St. Louis, MO, USA). CCl_4 treatment in 6–8 weeks old animals was performed twice weekly by intraperitoneal (i.p.) injection of 5 μl CCl_4 diluted 1:20 in corn oil. Five animals per group and condition were used. Experiments were performed at least 3 times. The hamster anti-murine CXCL10 mAb (1F11, [17]) was administered at 50 μg or 100 μg in 100 μl PBS per mouse three times a week starting 6 h before the first CCl_4 injection. As control, an isotype-matched hamster IgG Ab (Southern Biotechnology, Birmingham, AL, USA) was used. All animal experiments have been approved by the local Ethics Animal Review Board, Darmstadt, Germany.

2.2. HSC isolation

HSCs were isolated from mouse livers by the pronase–collagenase method and a 12% Nycodenz gradient (Sigma-Aldrich, St. Louis, MO, USA) as described in [36]. Isolated cells were cultured in DMEM supplemented with 10% fetal bovine serum, 2 mM glutamine and 1% antibiotic solution at 37 °C. HSC purity was determined by Oil red O staining, which showed the typical light microscopic appearance of lipid droplets (Fig. 1B, left panel).

2.3. RNase protection assay (RPA)

Either freshly isolated HSCs were used or HSCs were seeded in 6-well plates in DMEM supplemented with 10% fetal bovine serum, 2 mM glutamine and 1% antibiotic solution. The next day, cells were washed with PBS and serum-starved in DMEM supplemented with 1% bovine serum albumin and 1% antibiotic solution for 24 h. Then, cells were stimulated with IFNγ (PeproTech, London, UK) for indicated times. Total RNA was isolated using Trizol (Invitrogen, Karlsruhe, Germany) according to the manufacturer's protocol. Eight micrograms of total RNA was used for hybridization with a ^{32}P-UTP-labeled multitemplate set containing specific probes for various chemokines (Riboquant, mCK-5, BD Biosciences, San Diego, CA, USA). The RPA was conducted according to the manufacturer's guidelines. The resulting analytical acrylamide gel was scanned using a Pharos imaging system (Bio-Rad, Munich, Germany). Intensity of bands corresponding to protected mRNA was quantified using Quantity One Software (Bio-Rad, Munich, Germany) and GAPDH was a reference gene.

2.4. Immunohistochemistry

Livers were harvested at the times indicated, immersed in Tissue-Tek O.C.T. (Sakura Finetek, Zoeterwoude, Netherlands) and quick-frozen on dry ice. Seven μm sections were cut and fixed in EtOH at –20 °C and after washing in PBS an avidine-biotin blocking step (Vector laboratories, Burlingame, CA, USA) was included. Primary and biotinylated secondary antibodies (Vector laboratories, Burlingame, CA, USA) were incubated with the sections for 60 min each and color reaction was obtained by sequential incubation with avidine-peroxidase conjugate (Vector laboratories, Burlingame, CA, USA) and diaminobenzidine-hydrogen peroxide. Primary antibodies used were: rat anti-mouse CD4, rat anti-mouse CD8α, rat anti-mouse CD19 and rat anti-mouse CD45R/B220 mAbs (all from BD Biosciences, San Diego, CA, USA), rat anti-mouse F4/80 mAb (AbD Serotec, Raleigh, NC, USA), polyclonal rabbit anti-human desmin antibody (abcam, Cambridge, UK), rabbit anti-granzyme B antibody (abcam, Cambridge, UK), rabbit anti-Ki67 antibody (abcam, Cambridge, UK), biotinylated hamster anti-mouse CD11c mAb (eBioscience, San Diego, CA, USA), goat anti-NKp46 antibody (R&D Systems, Minneapolis, MN, USA) and

rabbit anti-mouse collagen I antibody (Chemicon, Temecula, USA). To visualize CXCL10 production in HSCs, starved cells were incubated in culture medium containing 0.5% FCS and 10 ng/ml IFNγ for 8 h, then medium was replaced and cells were treated with 10 ng/ml IFNγ and 2 μg/ml Brefeldin A for additional 15 h. Cells were fixed in 4% paraformaldehyde and CXCL10 was stained with a polyclonal rabbit anti-mouse CXCL10 antibody (PeproTech, London, UK), as described above. Staining of αSMA was done with a mouse anti-human αSMA mAb (1A4, DakoCytomation, Glostrup, Denmark) and the Vector MOM kit (Vector laboratories, Burlingame, CA, USA). Sirius Red staining was done by incubating EtOH-fixed cryosections for 1 h in Sirius Red solution containing 0.1% saturated picric acid (Electron Microscopy Sciences, Hatfield, PA, USA). Sections were washed in 2 changes of 0.01 N HCl for 2 min, rinsed in water, dehydrated in 3 changes of absolute EtOH for 1 min each, incubated in 2 changes of xylol and mounted in Roti-Histokitt (Roth, Karlsruhe, Germany). Relative fibrosis area, expressed as % of total liver area, was assessed by analyzing 7 liver sections per animal. Fields were acquired at ×10 magnification and then analyzed with the computerized morphometry system Quantity One (Bio-Rad, Munich, Germany). Results are mean ± SEM (n = 7).

2.5. Flow cytometry

HSCs isolated from 6 naïve mice or from 6 mice treated with CCl_4 for 4 weeks were kept in culture for 20 h and were then detached and washed. Cells were stained for surface expression of CXCR3 and were subsequently fixed, permeabilized and stained for intracellular GFAP as previously described [37]. APC-conjugated rat anti-mouse CXCR3 mAb was from R&D Systems (Minneapolis, MN, USA) and Alexa488-conjugated anti-GFAP mAb was from Chemicon (Temecula, USA). Samples were acquired using a FACS Canto II flow cytometer (BD Biosciences, Heidelberg, Germany).

2.6. Transwell migration assay

Freshly isolated HSCs were seeded in the upper chamber of a Transwell insert (8 μM pore size, Corning Costar, Chorges, France) at 200,000 cells/well in complete culture medium. The lower chamber was filled with medium supplemented with 20 ng/ml recombinant mouse CXCL10 (PeproTech, London, UK). Assays were incubated at 37 °C for up to 3 days. Medium ± CXCL10 in the lower chamber was replaced every day. To stop migration, cells were fixed in methanol and stained in crystal violet. Cells on the upper side of the membrane were wiped off with a cotton swap and cells that had migrated through the pores to the underside of the membrane were quantified. Of each filter, pictures of 10 individual fields were taken and cells were counted. Assays were done in duplicates and repeated 3 times. Results are mean ± SD (n = 3) per condition.

2.7. Protein immunoblotting

Total protein extracts were prepared in PBS containing 1% Triton X-100 and complete EDTA-free protease inhibitor cocktail (Roche Diagnostics, Mannheim, Germany). Proteins (100 μg/lane) were resolved on a 10% SDS-polyacrylamide gel. Immunoblots were incubated overnight at 4 °C with polyclonal rabbit anti-human desmin antibody (abcam, Cambridge, UK) or rabbit anti-GFAP antibody (DakoCytomation, Glostrup, Denmark) and sequentially with mouse anti-HSP70 mAb (abcam, Cambridge, UK). Alkaline phosphatase-conjugated secondary antibodies (Bio-Rad, Munich, Germany) were visualized with ECF substrate Vistra (Amersham Biosciences, Buckinghamshire, UK) and the Pharos FX Plus imager system (Bio-Rad, Munich, Germany). Livers of 2 wildtype and 2 $CXCL10^{-/-}$ animals were analyzed.

2.8. Serum aminotransferase assays

Activity assays for alanine aminotransferase and aspartate aminotransferase were performed with the RANDOX ALT/AST kit (RANDOX, Crumlin, UK). Sera of 5 mice per group were tested. Results are mean ± SD ($n = 5$) per condition.

2.9. Statistical analysis

The parametric data were analyzed by Student *t* test. Values of $P < 0.05$ were considered statistically significant.

3. Results

3.1. CXCL10 promotes liver fibrosis

Our initial studies in C57BL/6 mice showed an upregulation of CXCL10 mRNA in livers of mice that have been exposed to chronic CCl_4 treatment. A kinetic analysis of CXCL10 mRNA expression conducted in HSC enriched fractions obtained from pools of 5 livers of CCl_4-treated mice per time revealed an up to 10-fold upregulation of CXCL10 at the peak of expression (week 4 of treatment) (Fig. 1A). Next, we determined whether isolated HSCs (Fig. 1B) have the potential to produce CXCL10 *in vitro*. To this end, we treated serum-starved cells isolated from wildtype or CXCL10$^{-/-}$ mice with 10 ng/ml recombinant IFNγ and stained for intracellular CXCL10. In contrast to HSCs isolated from CXCL10$^{-/-}$ mice, wildtype HSCs readily produced CXCL10 within 24 h of stimulation (Fig. 1B). RNase protection assays revealed that wildtype HSCs expressed small amounts of CXCL10 mRNA constitutively, whereas no CXCL10 signal was detectable in CXCL10$^{-/-}$ HSCs (Fig. 1C). Upon IFNγ stimulation, wildtype HSCs time-dependently increased CXCL10 mRNA production, resulting in a more than 80-fold increase in CXCL10 message. There was no further increase in signal intensity when 100 ng/ml IFNγ were used (Fig. 1C).

To test the importance of CXCL10 in liver fibrosis, we compared wildtype mice with CXCL10$^{-/-}$ mice, which both were treated with CCl_4 for 4 weeks. Sirius red stainings revealed that in livers from wildtype mice periportal collagen deposition was substantial and bridging fibrosis was evident (Fig. 2A). In contrast, livers from CXCL10$^{-/-}$ mice only occasionally showed collagen fibers reaching from the periportal area deeper into the liver parenchyma and no signs of emerging bridging fibrosis were seen (Fig. 2A). More specifically, morphometric analysis revealed that hepatic fibrosis decreased from 5.03 ± 0.69% (mean ± SEM) in wildtype livers to 1.68 ± 0.32% in CXCL10$^{-/-}$ livers. To localize HSCs in these tissues, we performed immunohistochemical stainings in consecutive sections using an antibody to desmin to visualize both quiescent and activated HSCs and an antibody to αSMA to stain for activated HSCs. In livers obtained from CCl_4-treated CXCL10$^{-/-}$ mice, HSCs were mostly distributed around blood vessels with only low numbers showing parenchymal localization. The αSMA staining was rather weak, indicating that nearly all HSCs were in an inactive state (Fig. 2B and C). In livers of wildtype mice, desmin staining was much stronger and the majority of desmin-positive cells was also αSMA-positive (Fig. 2B and C). Activated HSCs were found in the perivascular region and extensively penetrated into the parenchyma, explaining the high content of Sirius red stained fibers in these regions (Fig. 2A). Thus, our data indicate that CCl_4 treatment triggers an upregulation of CXCL10 in the liver and that CXCL10 plays an important role in chemically induced liver fibrosis. In the absence of CXCL10, fibrosis is less severe.

3.2. Livers of naïve wildtype and CXCL10$^{-/-}$ mice show no difference in HSC levels and distribution. CCl_4-induced hepatocyte damage is similar in wildtype and CXCL10$^{-/-}$ mice

Next, we analyzed whether livers of naïve wildtype and CXCL10$^{-/-}$ mice show differences in HSC localization and/or content. Desmin staining revealed similar cell numbers and comparable HSC distribution (Fig. 3A) and immunoblotting demonstrated equal amounts of GFAP (marker for quiescent HSC) and desmin expressed in these livers (Fig. 3B). Hence, livers of naïve wildtype and CXCL10$^{-/-}$ mice show similar HSC-linked characteristics. Also, acute liver damage induced by CCl_4 is comparable in wildtype and CXCL10$^{-/-}$ mice: Activities of alanine – and aspartate aminotransferases (ALT/AST) were equally increased 4 h after the first CCl_4 injection and got back to control levels at day 4, right before the next CCl_4 injection was performed (Fig. 3C). After chronic treatment for 4 weeks, ALT and AST levels were still similar in wildtype and CXCL10$^{-/-}$ livers (Fig. 3C). Therefore, reduced fibrosis in CCl_4-treated CXCL10$^{-/-}$ livers cannot be explained by lower initial HSC numbers or higher hepatocyte resistance to chemical damage.

3.3. Quiescent HSCs express CXCR3 and CXCR3$^+$ HSCs are frequent in activated populations

HSCs may directly respond to a change in CXCL10 concentrations if they express the CXCL10-specific receptor CXCR3. Using flow cytometry, we tested cell surface expression of CXCR3 in HSCs isolated from livers of naïve control- or CCl_4-treated wildtype mice. Prior to analysis, HSCs were kept in culture for 20 h. HSC purity was >90% as determined by Oil red O staining (Fig. 1B, left panel). HSCs were identified by staining for intracellular expression of the HSC marker GFAP [38]. Fig. 3D shows that 8.6% of the analyzed GFAP-positive control HSCs were CXCR3$^+$. Interestingly, the number of GFAP$^+$ CXCR3$^+$ HSCs increased to 42.4% in cell preparations from livers purified after 4 weeks of CCl_4 treatment (Fig. 3D). These findings suggest that the frequency of CXCR3-expressing cells is higher in activated HSCs than in quiescent HSCs.

3.4. CXCL10 stimulates HSC migration but has not influence on HSC proliferation in vitro

To test whether CXCR3 expression has an influence on HSC migration, we performed chemotaxis assays. To this end, HSCs from control- or CCl_4-treated mice were isolated and seeded in Transwell migration chambers in the absence or presence of 20 ng/ml recombinant CXCL10. Medium in the lower chamber was replaced every 24 h. Migration was stopped after 1 day or 3 days of incubation and cells that had migrated to the underside of the Transwell membrane were stained and counted. Apparently, CXCL10 triggered increased migration in control HSCs whereas motility of CCl_4-exposed HSCs was not further amplified by CXCL10 (Fig. 4A).

Besides migration, CXCL10 could also influence HSC growth. However, when freshly isolated wildtype HSCs were treated with CXCL10, as described in the migration assay, there was no difference in proliferation measurable compared to untreated HSCs (data not shown). Thus, CXCL10 can stimulate migration but not proliferation of HSCs *in vitro*. To analyze proliferation *in vivo*, we stained Ki67 in CCl_4-treated livers of wildtype and CXCL10$^{-/-}$ mice. In livers of CXCL10$^{-/-}$ mice, Ki67 staining was mostly seen in hepatocytes and there was no increased proliferation apparent in fibrotic areas (Fig. 4B, left panels). In livers of wildtype mice, Ki67-positive cells were again hepatocytes but also infiltrating leukocytes (Fig. 4B, right panels, arrowheads). However, Ki67 signal was low in fibrotic regions with small numbers of infiltrating cells in both wildtype (Fig. 4B, right panels, arrows) and CXCL10$^{-/-}$ mice. This indicates that reduced fibrosis in CXCL10$^{-/-}$ livers is not due to a lower proliferation capacity of HSCs in the absence of CXCL10, as CXCL10 rather influences HSC migration than HSC growth.

3.5. CXCL10 promotes lymphocyte migration into the liver

We next investigated whether the absence of CXCL10 in the knock-out animals may have an effect on the recruitment of CXCR3-expressing immune cells, such as activated T cells, DCs or B lymphocytes. Indeed, histological examinations revealed large clusters of $B220^+$ cells in livers of CCl_4-treated wildtype mice (Fig. 5A), whereas only small groups of $B220^+$ cells were visible in livers of $CXCL10^{-/-}$ mice (Fig. 5B). Overall, CD4 T cells were less prominent after CCl_4 administration than $B220^+$ cells, but the number of infiltrating CD4 T cells was significantly reduced in livers of $CXCL10^{-/-}$ mice compared to livers of wildtype animals (Fig. 5C and D). There were hardly any infiltrating CD8 T lymphocytes detectable after CCl_4 treatment in both $CXCL10^{-/-}$ and wildtype mice (data not shown). In addition, there was no difference in the frequency of $F4/80^+$ cells between $CXCL10^{-/-}$ and wildtype mice, which was possibly due to the relative abundance of $F4/80^+$ liver resident Kupffer cells (data not shown). Quantitative analysis of the stained sections showed that in livers of CCl_4-treated $CXCL10^{-/-}$ mice the number of $B220^+$ and $CD4^+$ cells was reduced to approximately 37% and 51% compared to livers of wildtype mice, respectively (Fig. 5E). Since B220 is expressed by B lymphocytes as well as by DCs, we also stained with mAbs to CD19 (B cell marker) and CD11c (marker for DCs). Both cell types were less abundant in $CXCL10^{-/-}$ animals than in wildtype mice (Fig. 5E). These results indicate that CXCL10 is required for an efficient attraction of B cells, DCs and CD4 T cells.

3.6. Anti-CXCL10 therapy protects from CCl_4-induced liver fibrosis

We then addressed the question whether therapeutic blocking of CXCL10 using a neutralizing anti-CXCL10 mAb could prevent liver fibrosis caused by CCl_4. Therefore, we injected 50 mg or 100 mg anti-CXCL10 mAb or an isotype-mached control IgG into wildtype animals three times a week starting at 6 h before beginning of CCl_4 administration and lasting for 4 weeks. When analyzing collagen deposition it became apparent that CXCL10 blockade reduced liver fibrosis drastically (Fig. 6A). Morphometric analysis revealed that hepatic fibrosis decreased from 5.02 ± 0.19% (mean ± SEM) in control livers to 1.05 ± 0.13% in anti-CXCL10 mAb treated livers. In addition, lower numbers of activated HSCs were visible in livers of anti-CXCL10 mAb treated mice (Fig. 6B). Furthermore, the numbers of infiltrating $B220^+$ cells and CD4 T cells were strongly reduced in an anti-CXCL10 mAb concentration dependent manner (Fig. 6C). In fact, 100 μg mAb per mouse were as effective in blocking lymphocyte infiltration as a complete knock-out of the CXCL10 gene. Our data provide evidence that blockade of CXCL10 by a suitable antibody decreases cellular infiltration into the liver, which in turn may reduce fibrosis formation.

3.7. Increased NK presence in the absence of CXCL10 protects from liver fibrosis

Since CXCR3 is prominently expressed on NK cells, we further wanted to investigate how CXCL10 influences NK cells during chronic CCl_4 exposure. Interestingly, staining of liver sections with an antibody to the NK marker NKp46 showed that in the absence of CXCL10, either due to genetic deletion ($CXCL10^{-/-}$ mice; Fig. 7A, middle panel) or antibody neutralization (blocking anti-CXCL10 mAb; Fig. 7A, right panel) the number of infiltrating NK cells is more than 7-fold higher (Fig. 7A) than in wildtype livers, after 4 weeks of CCl_4 treatment (Fig. 7A, left panel). Since it is known that NK cells can kill activated HSCs [39,40], we next determined the level of αSMA expression in consecutive sections. Indeed, activated HSCs were only numerous in CCl_4-treated control livers, in areas where NKp46 staining was weak (Fig. 7A, left panel). However, in CCl_4-exposed livers of $CXCL10^{-/-}$ mice or wildtype mice treated with the blocking anti-CXCL10 IgG, αSMA levels were low (Fig. 7A, middle and right panels), correlating with the reduced fibrosis observed in such livers (Fig. 2A and Fig. 6A). These findings indicate that $CXCL10^{-/-}$ mice are protected from CCl_4-induced liver fibrosis due to a higher rate of NK cell infiltration, which might be responsible for the observed reduction in the frequency of activated HSCs. NK cells kill

activated HSCs by a classical mechanism involving perforin and granzyme B [41]. Analyzing consecutive sections of CCl_4-treated wildtype livers, we detected moderate granzyme B expression but high αSMA levels in areas with NK presence (Fig. 7B, upper panels). However, in CXCL10$^{-/-}$ livers, granzyme B expression was high in regions with elevated NK cell content and low numbers of αSMA-positive HSCs. (Fig. 7B, lower panels). Taken together, our results suggest that the lower frequency of activated HSCs observed in CXCL10$^{-/-}$ livers is due to HSC killing by NK-triggered granzyme B-dependent cytotoxicity, resulting in reduced liver fibrosis.

4. Discussion

We report that in the absence of CXCL10, CCl_4-induced liver fibrosis is less severe and that recruitment of CD4 T cells, DCs and B220$^+$ cells to the affected liver is strongly reduced. In contrast, the number of infiltrating NK cells is massively increased in both CXCL10$^{-/-}$ mice as well as in wildtype C57BL/6 mice treated with neutralizing anti-CXCL10 antibody. Furthermore, we show that HSCs express CXCR3 and respond to CXCL10 with an increase in motility. Interestingly, HSCs secrete CXCL10 upon IFNγ stimulation. Our findings suggest that HSCs and a subset of CXCR3$^+$ immune cells are attracted to sites of liver damage by CXCL10. Relocated HSCs themselves may secrete CXCL10 and thus may subsequently further increase liver infiltration.

Previous studies documented that in both man and mouse chronic liver damage by toxic injury, pathogens or autoimmune liver disorders caused an increase in CXCL10 expression. Importantly, these CXCL10 levels correlated with the degree of inflammation [24–30]. Therefore, it is not surprising that we found an increase in CXCL10 mRNA in CCl_4-exposed mouse livers.

Hepatocytes are a major source of CXCL10 in the liver. In chronic hepatitis B and C, as well as in AIH and PBC patients but not in control individuals, lobular hepatocytes expressed CXCL10 and attracted infiltrating CXCR3$^+$ lymphocytes [25–27]. Furthermore, primary rat hepatocytes secreted CXCL10 after stimulation with IFNγ [42]. Importantly, the hepatocyte cell line AML-12 expressed CXCL10 when exposed to CCl_4 [30], suggesting a direct parenchymal response to cellular injury before inflammatory cells have even reached the site of damage. The finding that mouse HSCs express CXCR3 and respond to CXCL10 with increased motility (our observation and [43]) might be one reason why we observed a more pronounced clustering of HSCs (stronger desmin staining) in wildtype than CXCL10$^{-/-}$ portal areas where damaged hepatocytes are predominantly located. Attracted HSCs might then be activated by hepatocytes, leading to upregulation of αSMA expression, which was in our studies indeed stronger in livers of CCl_4-treated wildtype than CXCL10$^{-/-}$ mice. Interestingly, we found in addition that HSCs upregulated CXCL10 expression when they were stimulated by IFNγ *in vitro*. This finding indicates that HSCs attracted to damaged hepatocytes might be further stimulated to secret CXCL10 by infiltrating T cells producing IFNγ. This points to a complex crosstalk between immune cells and HSCs and supports data presented by Holt et al. showing that human HSCs regulate lymphocyte migration and adhesion *in vitro* [44].

It is well established in various disease models that CXCL10 is required to recruit different types of immune cells to the site of tissue damage and that it plays a key role in inflammation and autoimmunity [13–15,17,45–50]. CXCL10$^{-/-}$ mice are born with an intact immune system. However, they show an impaired T cell response with reduced T cell proliferation and T cell infiltration into inflamed tissue in reply to antigenic challenge [16]. When we treated CXCL10$^{-/-}$ mice with CCl_4, we observed reduced invasion of B cells, DCs as well as CD4 T cells, whereas the number of recruited CD8 T cells was similar than in

wildtype animals. The importance of $CD19^+$ $B220^+$ B cells in liver disease has been documented by Novobrantseva et al. [51]. In a model of CCl_4-induced liver damage, B cell-deficient mice showed reduced fibrosis and this effect was antibody independent. It seemed that in the absence of B cells, $F4/80^+$ macrophages were more efficient in removing dying hepatocytes, resulting in a lower number of activated HSCs and thus reduced collagen deposition [51]. In addition, one can speculate that activated B cells themselves could act on HSCs by release of cytokines. Further, CD4 T cells alone played no important role in CCl_4-induced liver injury, because fibrosis in mice lacking CD4 Tcells was as severe as in wildtype mice [51]. Thus, our observation that less CD4 T cells have been found in livers of $CXCL10^{-/-}$ mice than wildtype animals might be the consequence of B cell absence rather than the cause for reduced fibrosis.

The most intriguing observation of our study might be the increase in NK cell numbers in CCl_4-exposed $CXCL10^{-/-}$ livers. It has been previously shown that NK cells express CXCR3 and neutralization of CXCL9 and CXCL10 reduced the recruitment of NK cells to the liver after Hepatitis B virus infection [52]. In Con A induced hepatitis, NK recruitment from the circulation into the liver was macrophage inflammatory protein 1α (MIP-1α) dependent. However, the initial mobilization of NK cells from the spleen into the circulation was triggered by CXCL9 but not by CXCL10 [53]. Given the fact that CXCL9 is a less potent ligand than CXCL10 [54], one can imagine that in the absence of CXCL10, the effect of CXCL9 is stronger than normal, since competition between both ligands for binding to CXCR3 does no longer apply. Thus, CXCL9 has a higher potential to mobilize NK cells in $CXCL10^{-/-}$ mice than in wildtype animals. In SCID-BEIGE mice, which lack NK cells (in addition to absence of B cells and T cells), CCl_4 treatment triggered stronger fibrosis than in SCID mice (lacking B- and T cells), again underscoring the anti-fibrotic potential of NK cells [55]. Importantly, NK cell activities negatively correlated with liver fibrosis in patients with chronic hepatitis C infection [40]. The anti-fibrotic effect of NK cells has been demonstrated to be mediated by their capability to specifically kill early-activated but not quiescent HSCs [39,41,55]. HSC killing was induced due to upregulation of the NK cell activating ligand retinoic acid early inducible gene 1 (RAE-1) and involved perforin/granzyme B-dependent cytotoxicity [41,56]. Also in our experiments, activated HSC were the target of granzyme B-linked cell death.

Finally, it is an important finding that the treatment with a neutralizing anti-CXCL10 mAb was successful in significantly reducing hepatic fibrosis. Thus, the development of reagents to manipulate the CXCL10/CXCR3 trafficking pathway may be a useful therapeutic strategy to decrease liver fibrosis. However, such reagents need to be highly specific for the CXCL10 pathway, as $CXCR3^{-/-}$ mice showed increased liver fibrosis when exposed to CCl_4 [57]. In absence of CXCR3, CXCL9 might no longer be able to recruit NK cells and as a consequence activated HSCs would further promote liver fibrosis. Interestingly, the pro-fibrotic role of CXCL10 seems to be liver-specific, as pulmonary fibrosis was more severe in bleomycin-treated $CXCL10^{-/-}$ mice than in wildtype animals [58]. In this fibrosis model, CXCL10 inhibited fibroblast migration, whereas leukocyte recruitment was not affected. Thus, depending on the organ, different cell types may be the target of CXCL10 controlled motility resulting in an organ-specific impact of CXCL10 on fibrosis.

In the future it will be important to investigate the role of CXCL10 and the therapeutic potential of its neutralization in hepatic fibrosis occurring as a consequence of autoimmune liver diseases or chronic viral infection, such as Hepatitis B or C virus infection. Novel model systems, like the cytochrome P450 2D6 (CYP2D6) mouse model, which uses an adenovirus expressing the major human autoantigen CYP2D6 to induce autoimmune hepatitis [59], might be an excellent tool to follow the development of hepatic fibrosis from

the initiation of autoimmunity by adenovirus-CYP2D6 infection to the final stages of autoimmune liver destruction.

Acknowledgments

This work is supported by NIH grant R21 DK071577 and a grant of the German Research Foundation to U.C. and NIH grant R01-CA069212 to A.D.L.

Abbreviations

AIH	autoimmune hepatitis
αSMA	α-smooth muscle actin
CCl_4	carbon tetrachloride
DC	dendritic cell
ECM	extracellular matrix
HSC	hepatic stellate cell
mAb	monoclonal antibody
NK	natural killer
PBC	primary biliary cirrhosis
PSC	primary sclerosing cholangitis
RPA	RNase protection assay

References

1. Bataller R, Brenner DA. Liver fibrosis. J Clin Invest. 2005; 115:209–18. [PubMed: 15690074]
2. Friedman SL, Rockey DC, Bissell DM. Hepatic fibrosis 2006: report of the Third AASLD Single Topic Conference. Hepatology. 2007; 45:242–9. [PubMed: 17187439]
3. Iredale JP. Models of liver fibrosis: exploring the dynamic nature of inflammation and repair in a solid organ. J Clin Invest. 2007; 117:539–48. [PubMed: 17332881]
4. Cheung O, Sanyal AJ. Recent advances in nonalcoholic fatty liver disease. Curr Opin Gastroenterol. 2009; 25:230–7. [PubMed: 19396962]
5. Czaja AJ. Autoimmune liver disease. Curr Opin Gastroenterol. 2009; 25:215–22. [PubMed: 19387256]
6. Jiao J, Friedman SL, Aloman C. Hepatic fibrosis. Curr Opin Gastroenterol. 2009; 25:223–9. [PubMed: 19396960]
7. Selmi C, Lleo A, Pasini S, Zuin M, Gershwin ME. Innate immunity and primary biliary cirrhosis. Curr Mol Med. 2009; 9:45–51. [PubMed: 19199941]
8. Vergani D, Mieli-Vergani G. Autoimmune Hepatitis and PSC Connection. Clin Liver Dis. 2008; 12:187–202. x. [PubMed: 18242504]
9. Friedman SL. Molecular regulation of hepatic fibrosis, an integrated cellular response to tissue injury. J Biol Chem. 2000; 275:2247–50. [PubMed: 10644669]
10. Gressner AM, Weiskirchen R. Modern pathogenetic concepts of liver fibrosis suggest stellate cells and TGF-beta as major players and therapeutic targets. J Cell Mol Med. 2006; 10:76–99. [PubMed: 16563223]
11. Svegliati-Baroni G, De Minicis S, Marzioni M. Hepatic fibrogenesis in response to chronic liver injury: novel insights on the role of cell-to-cell interaction and transition. Liver Int. 2008; 28:1052–64. [PubMed: 18783548]
12. Winau F, Quack C, Darmoise A, Kaufmann SH. Starring stellate cells in liver immunology. Curr Opin Immunol. 2008; 20:68–74. [PubMed: 18068343]

13. Christen U, McGavern DB, Luster AD, von Herrath MG, Oldstone MB. Among CXCR3 chemokines, IFN-gamma-inducible protein of 10 kDa (CXC chemokine ligand (CXCL) 10) but not monokine induced by IFN-gamma (CXCL9) imprints a pattern for the subsequent development of autoimmune disease. J Immunol. 2003; 171:6838–45. [PubMed: 14662890]
14. Rhode A, Pauza ME, Barral AM, Rodrigo E, Oldstone MB, von Herrath MG, et al. Islet-specific expression of CXCL10 causes spontaneous islet infiltration and accelerates diabetes development. J Immunol. 2005; 175:3516–24. [PubMed: 16148094]
15. Christen U, Benke D, Wolfe T, Rodrigo E, Rhode A, Hughes AC, et al. Cure of prediabetic mice by viral infections involves lymphocyte recruitment along an IP-10 gradient. J Clin Invest. 2004; 113:74–84. [PubMed: 14702111]
16. Dufour JH, Dziejman M, Liu MT, Leung JH, Lane TE, Luster AD. IFN-gamma-inducible protein 10 (IP-10; CXCL10)-deficient mice reveal a role for IP-10 in effector T cell generation and trafficking. J Immunol. 2002; 168:3195–204. [PubMed: 11907072]
17. Khan IA, MacLean JA, Lee FS, Casciotti L, DeHaan E, Schwartzman JD, et al. IP-10 is critical for effector T cell trafficking and host survival in *Toxoplasma gondii* infection. Immunity. 2000; 12:483–94. [PubMed: 10843381]
18. Arai K, Liu ZX, Lane T, Dennert G. IP-10 and Mig facilitate accumulation of T cells in the virus-infected liver. Cell Immunol. 2002; 219:48–56. [PubMed: 12473267]
19. Oo YH, Adams DH. The role of chemokines in the recruitment of lymphocytes to the liver. J Autoimmun. 2010; 34:45–54. [PubMed: 19744827]
20. Clark-Lewis I, Mattioli I, Gong JH, Loetscher P. Structure-function relationship between the human chemokine receptor CXCR3 and its ligands. J Biol Chem. 2003; 278:289–95. [PubMed: 12417585]
21. Kohrgruber N, Groger M, Meraner P, Kriehuber E, Petzelbauer P, Brandt S, et al. Plasmacytoid dendritic cell recruitment by immobilized CXCR3 ligands. J Immunol. 2004; 173:6592–602. [PubMed: 15557149]
22. Bonecchi R, Bianchi G, Bordignon PP, D'Ambrosio D, Lang R, Borsatti A, et al. Differential expression of chemokine receptors and chemotactic responsiveness of type 1 T helper cells (Th1s) and Th2s. J Exp Med. 1998; 187:129–34. [PubMed: 9419219]
23. Garcia-Lopez MA, Sanchez-Madrid F, Rodriguez-Frade JM, Mellado M, Acevedo A, Garcia MI, et al. CXCR3 chemokine receptor distribution in normal and inflamed tissues: expression on activated lymphocytes, endothelial cells, and dendritic cells. Lab Invest. 2001; 81:409–18. [PubMed: 11310833]
24. Asselah T, Bieche I, Laurendeau I, Paradis V, Vidaud D, Degott C, et al. Liver gene expression signature of mild fibrosis in patients with chronic hepatitis C. Gastroenterology. 2005; 129:2064–75. [PubMed: 16344072]
25. Harvey CE, Post JJ, Palladinetti P, Freeman AJ, Ffrench RA, Kumar RK, et al. Expression of the chemokine IP-10 (CXCL10) by hepatocytes in chronic hepatitis C virus infection correlates with histological severity and lobular inflammation. J Leukoc Biol. 2003; 74:360–9. [PubMed: 12949239]
26. Nishioji K, Okanoue T, Itoh Y, Narumi S, Sakamoto M, Nakamura H, et al. Increase of chemokine interferon-inducible protein-10 (IP-10) in the serum of patients with autoimmune liver diseases and increase of its mRNA expression in hepatocytes. Clin Exp Immunol. 2001; 123:271–9. [PubMed: 11207658]
27. Zeremski M, Petrovic LM, Chiriboga L, Brown QB, Yee HT, Kinkhabwala M, et al. Intrahepatic levels of CXCR3-associated chemokines correlate with liver inflammation and fibrosis in chronic hepatitis C. Hepatology. 2008
28. Chuang YH, Lian ZX, Cheng CM, Lan RY, Yang GX, Moritoki Y, et al. Increased levels of chemokine receptor CXCR3 and chemokines IP-10 and MIG in patients with primary biliary cirrhosis and their first degree relatives. J Autoimmun. 2005; 25:126–32. [PubMed: 16243485]
29. Itoh Y, Morita A, Nishioji K, Fujii H, Nakamura H, Kirishima T, et al. Time course profile and cell-type-specific production of monokine induced by interferon-gamma in Concanavalin A-induced hepatic injury in mice: comparative study with interferon-inducible protein-10. Scand J Gastroenterol. 2001; 36:1344–51. [PubMed: 11761028]

30. Koniaris LG, Zimmers-Koniaris T, Hsiao EC, Chavin K, Sitzmann JV, Farber JM. Cytokine-responsive gene-2/IFN-inducible protein-10 expression in multiple models of liver and bile duct injury suggests a role in tissue regeneration. J Immunol. 2001; 167:399–406. [PubMed: 11418676]

31. Bone-Larson CL, Hogaboam CM, Evanhoff H, Strieter RM, Kunkel SL. IFN-gamma-inducible protein-10 (CXCL10) is hepatoprotective during acute liver injury through the induction of CXCR2 on hepatocytes. J Immunol. 2001; 167:7077–83. [PubMed: 11739529]

32. Hogaboam CM, Bone-Larson CL, Steinhauser ML, Lukacs NW, Colletti LM, Simpson KJ, et al. Novel CXCR2-dependent liver regenerative qualities of ELR-containing CXC chemokines. FASEB J. 1999; 13:1565–74. [PubMed: 10463948]

33. Yoneyama H, Kai Y, Koyama J, Suzuki K, Kawachi H, Narumi S, et al. Neutralization of CXCL10 accelerates liver regeneration in carbon tetrachloride-induced acute liver injury. Med Mol Morphol. 2007; 40:191–7. [PubMed: 18085377]

34. Tiegs G, Hentschel J, Wendel A. A T cell-dependent experimental liver injury in mice inducible by concanavalin A. J Clin Invest. 1992; 90:196–203. [PubMed: 1634608]

35. Nagy LE. Recent insights into the role of the innate immune system in the development of alcoholic liver disease. Exp Biol Med (Maywood). 2003; 228:882–90. [PubMed: 12968059]

36. Proell V, Mikula M, Fuchs E, Mikulits W. The plasticity of p19 ARF null hepatic stellate cells and the dynamics of activation. Biochim Biophys Acta. 2005; 1744:76–87. [PubMed: 15878400]

37. Christen U, Wolfe T, Mohrle U, Hughes AC, Rodrigo E, Green EA, et al. A dual role for TNF-alpha in type 1 diabetes: islet-specific expression abrogates the ongoing autoimmune process when induced late but not early during pathogenesis. J Immunol. 2001; 166:7023–32. [PubMed: 11390446]

38. Winau F, Hegasy G, Weiskirchen R, Weber S, Cassan C, Sieling PA, et al. Ito cells are liver-resident antigen-presenting cells for activating T cell responses. Immunity. 2007; 26:117–29. [PubMed: 17239632]

39. Gao B, Radaeva S, Jeong WI. Activation of natural killer cells inhibits liver fibrosis: a novel strategy to treat liver fibrosis. Expert Rev Gastroenterol Hepatol. 2007; 1:173–80. [PubMed: 19072444]

40. Notas G, Kisseleva T, Brenner D. NK and NKT cells in liver injury and fibrosis. Clin Immunol. 2009; 130:16–26. [PubMed: 18823822]

41. Radaeva S, Sun R, Jaruga B, Nguyen VT, Tian Z, Gao B. Natural killer cells ameliorate liver fibrosis by killing activated stellate cells in NKG2D-dependent and tumor necrosis factor-related apoptosis-inducing ligand-dependent manners. Gastroenterology. 2006; 130:435–52. [PubMed: 16472598]

42. Ren X, Kennedy A, Colletti LM. CXC chemokine expression after stimulation with interferon-gamma in primary rat hepatocytes in culture. Shock. 2002; 17:513–20. [PubMed: 12069190]

43. Bonacchi A, Romagnani P, Romanelli RG, Efsen E, Annunziato F, Lasagni L, et al. Signal transduction by the chemokine receptor CXCR3: activation of Ras/ERK, Src, and phosphatidylinositol 3-kinase/Akt controls cell migration and proliferation in human vascular pericytes. J Biol Chem. 2001; 276:9945–54. [PubMed: 11136732]

44. Holt AP, Haughton EL, Lalor PF, Filer A, Buckley CD, Adams DH. Liver myofibroblasts regulate infiltration and positioning of lymphocytes in human liver. Gastroenterology. 2009; 136:705–14. [PubMed: 19010327]

45. Fife BT, Kennedy KJ, Paniagua MC, Lukacs NW, Kunkel SL, Luster AD, et al. CXCL10 (IFN-gamma-inducible protein-10) control of encephalitogenic CD4+ T cell accumulation in the central nervous system during experimental autoimmune encephalomyelitis. J Immunol. 2001; 166:7617–24. [PubMed: 11390519]

46. Liu MT, Keirstead HS, Lane TE. Neutralization of the chemokine CXCL10 reduces inflammatory cell invasion and demyelination and improves neurological function in a viral model of multiple sclerosis. J Immunol. 2001; 167:4091–7. [PubMed: 11564831]

47. Shields PL, Morland CM, Salmon M, Qin S, Hubscher SG, Adams DH. Chemokine and chemokine receptor interactions provide a mechanism for selective T cell recruitment to specific liver compartments within hepatitis C-infected liver. J Immunol. 1999; 163:6236–43. [PubMed: 10570316]

48. Tamaru M, Nishioji K, Kobayashi Y, Watanabe Y, Itoh Y, Okanoue T, et al. Liver-infiltrating T lymphocytes are attracted selectively by IFN-inducible protein-10. Cytokine. 2000; 12:299–308. [PubMed: 10805209]
49. Christen U, von Herrath MG. Cytokines and chemokines in virus-induced autoimmunity. Adv Exp Med Biol. 2003; 520:203–20. [PubMed: 12613580]
50. Christen U, von Herrath MG. IP-10 and type 1 diabetes: a question of time and location. Autoimmunity. 2004; 37:273–82.
51. Novobrantseva TI, Majeau GR, Amatucci A, Kogan S, Brenner I, Casola S, et al. Attenuated liver fibrosis in the absence of B cells. J Clin Invest. 2005; 115:3072–82. [PubMed: 16276416]
52. Kakimi K, Lane TE, Wieland S, Asensio VC, Campbell IL, Chisari FV, et al. Blocking chemokine responsive to gamma-2/interferon (IFN)-gamma inducible protein and monokine induced by IFN-gamma activity in vivo reduces the pathogenetic but not the antiviral potential of hepatitis B virus-specific cytotoxic T lymphocytes. J Exp Med. 2001; 194:1755–66. [PubMed: 11748277]
53. Wald O, Weiss ID, Wald H, Shoham H, Bar-Shavit Y, Beider K, et al. IFN-gamma acts on T cells to induce NK cell mobilization and accumulation in target organs. J Immunol. 2006; 176:4716–29. [PubMed: 16585565]
54. Sauty A, Colvin RA, Wagner L, Rochat S, Spertini F, Luster AD. CXCR3 internalization following T cell-endothelial cell contact: preferential role of IFN-inducible T cell alpha chemoattractant (CXCL11). J Immunol. 2001; 167:7084–93. [PubMed: 11739530]
55. Melhem A, Muhanna N, Bishara A, Alvarez CE, Ilan Y, Bishara T, et al. Antifibrotic activity of NK cells in experimental liver injury through killing of activated HSC. J Hepatol. 2006; 45:60–71. [PubMed: 16515819]
56. Radaeva S, Wang L, Radaev S, Jeong WI, Park O, Gao B. Retinoic acid signaling sensitizes hepatic stellate cells to NK cell killing via upregulation of NK cell activating ligand RAE1. Am J Physiol Gastrointest Liver Physiol. 2007; 293:G809–16. [PubMed: 17673545]
57. Wasmuth HE, Lammert F, Zaldivar MM, Weiskirchen R, Hellerbrand C, Scholten D, et al. Antifibrotic effects of CXCL9 and its receptor CXCR3 in livers of mice and humans. Gastroenterology. 2009; 137:309–19. 319e1–319e3. [PubMed: 19344719]
58. Tager AM, Kradin RL, LaCamera P, Bercury SD, Campanella GS, Leary CP, et al. Inhibition of pulmonary fibrosis by the chemokine IP-10/CXCL10. Am J Respir Cell Mol Biol. 2004; 31:395–404. [PubMed: 15205180]
59. Holdener M, Hintermann E, Bayer M, Rhode A, Rodrigo E, Hintereder G, et al. Breaking tolerance to the natural human liver autoantigen cytochrome P450 2D6 by virus infection. J Exp Med. 2008; 205:1409–22. [PubMed: 18474629]

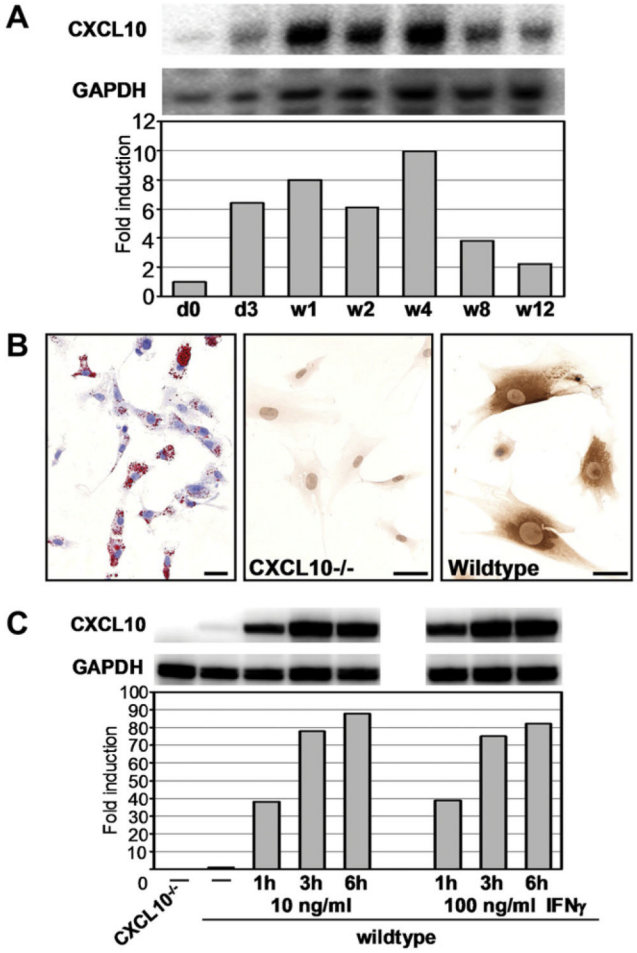

Fig. 1.

HSC enriched cell pools express CXCL10 after chronic CCl_4 treatment or upon IFNγ stimulation *in vitro*. (A) RNase protection assay using total RNA isolated from HSCs of C57BL/6 mice treated with CCl_4 for indicated time points. To prepare a HSC enriched cell pool, livers of 5 animals per time point were subjected to collagenase/pronase digest, followed by density gradient cell separation. The bar graph represents the quantification of relative amounts of CXCL10 mRNA normalized to signal intensities of GAPDH mRNA in each cell pool. Depicted is fold induction with time point d0 set at 1. (B and C) HSC pools have been isolated from 6 CXCL10$^{-/-}$ or 6 wildtype C57BL/6 mice. (B) Left panel: Oil Red O staining revealed a HSC purity of our preps of >90%. Central panel: Upon IFNγ stimulation (10 ng/ml) for 24 h, CXCL10$^{-/-}$ HSCs produced no CXCL10. Right panel: Wildtype HSCs secreted CXCL10 upon IFNγ stimulation. Scale bar = 20 μm. (C) Cultured HSCs were left untreated or were stimulated with IFNγ at 10 ng/ml or 100 ng/ml for indicated time points before total RNA was purified. CXCL10 or GAPDH encoding mRNA was analyzed by RPA. Signals have been normalized to the unstimulated wildtype control. Representative of $n = 3$.

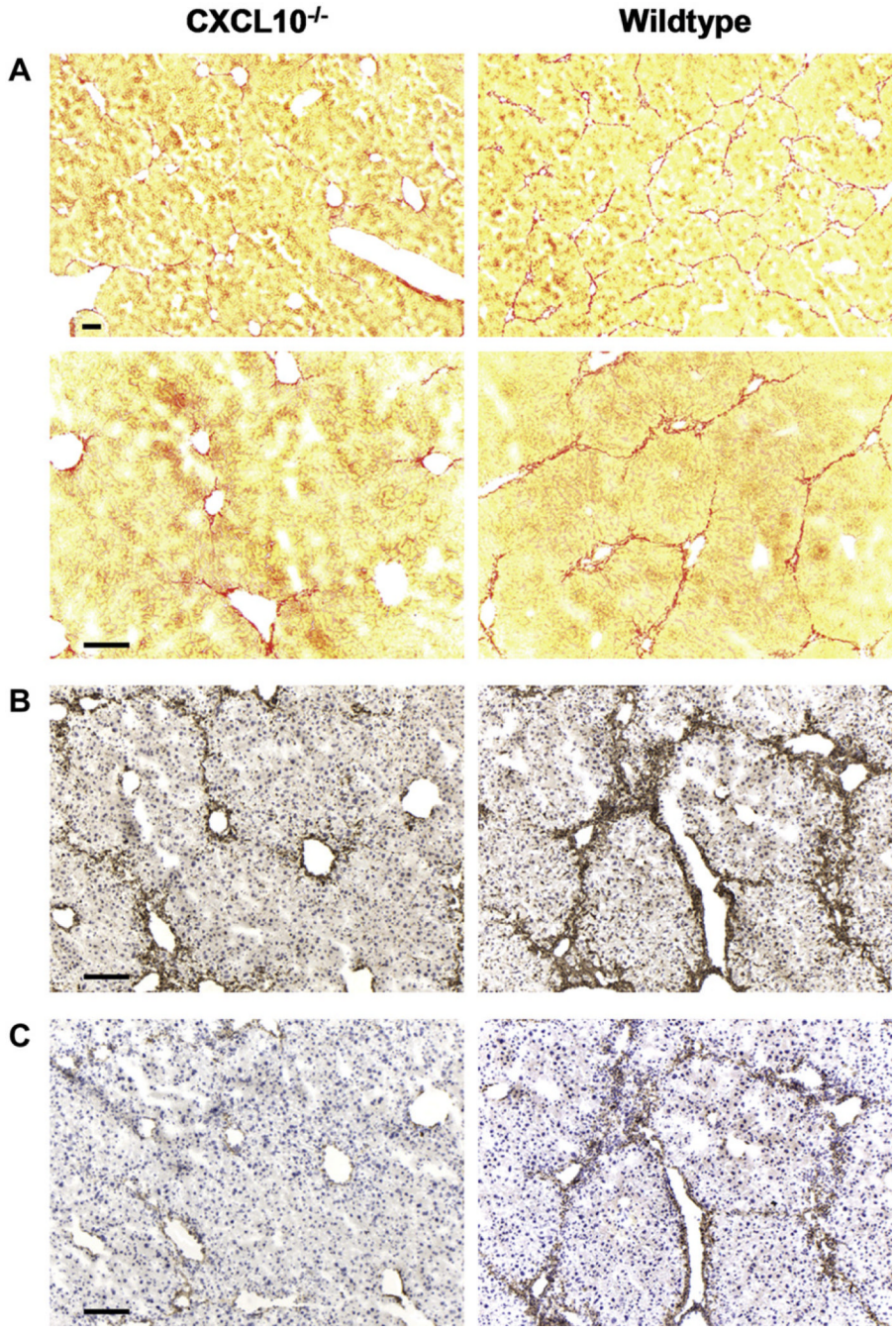

Fig. 2.

CXCL10$^{-/-}$ mice are protected from CCl_4-induced fibrosis. (A) Livers of CXCL10$^{-/-}$ and wildtype mice have been harvested after 4 weeks of CCl_4 treatment. Cryosections were stained with Sirius Red to visualize collagen fibers (two different magnifications are shown). Note that bridging fibrosis can only be seen in livers of wildtype but not of CXCL10$^{-/-}$ mice. To localize HSCs, consecutive sections from the identical livers were also stained with antibodies to (B) desmin and (C) αSMA. Total HSC staining (desmin, B) and staining of activated HSCs (αSMA, C) is much weaker in the absence of CXCL10 than in livers of wildtype animals. Scale bar = 100 μm. Representative of $n = 8$.

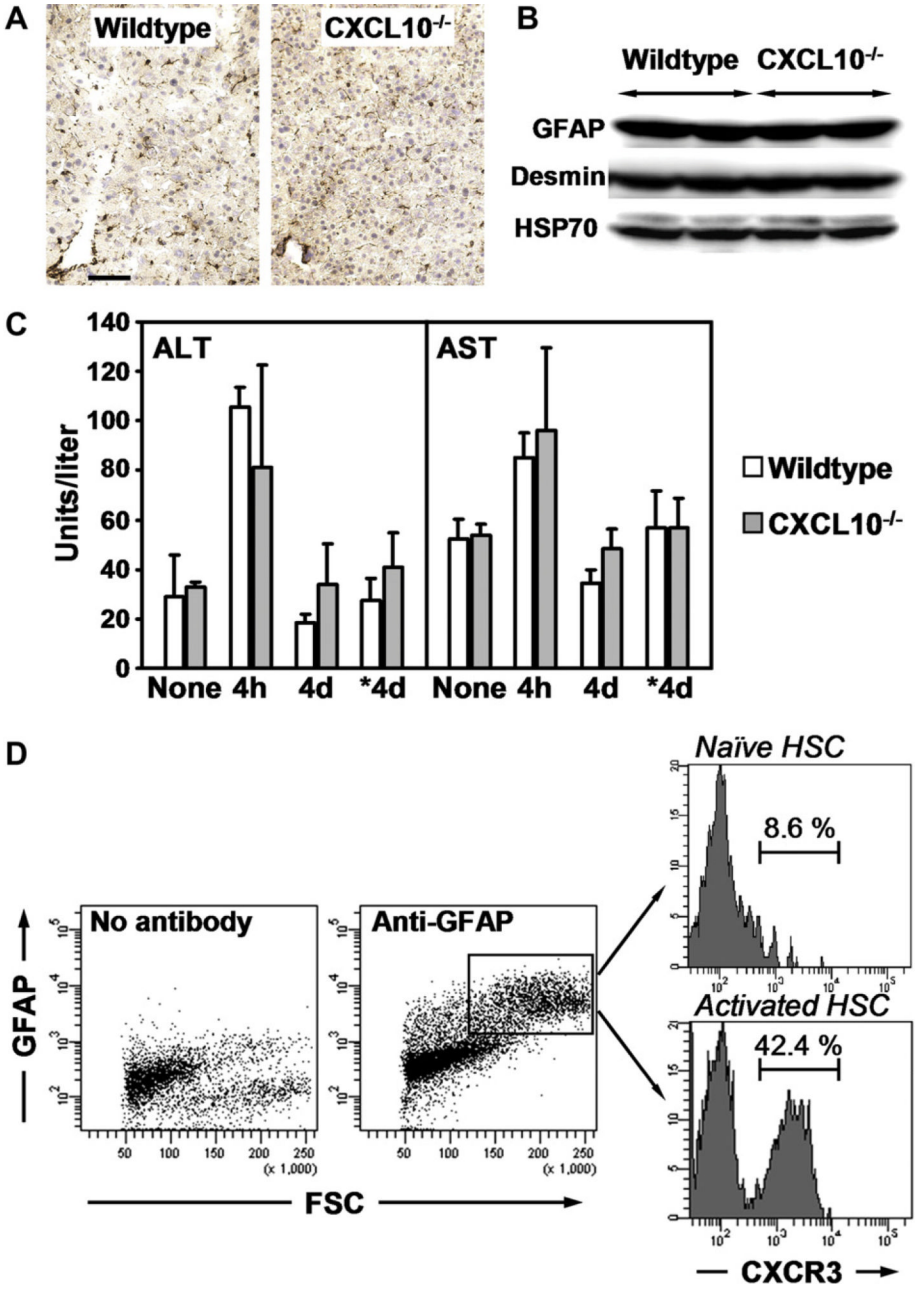

Fig. 3.

Wildtype and CXCL10$^{-/-}$ livers are similar in terms of initial HSC numbers and hepatocyte damage by CCl_4. HSCs express CXCR3 and the frequency of CXCR3 + HSCs increases upon stimulation. (A) Desmin staining of liver sections of naïve wildtype and CXCL10$^{-/-}$ mice. Scale bar = 50 μm. (B) Immunoblotting of equal amounts of total liver homogenates with antibodies to GFAP, desmin and HSP70. Two naïve animals per group were analyzed. (C) ALT and AST activities in sera from wildtype and CXCL10$^{-/-}$ mice. Sera were collected 4 h or 4 days after first CCl_4 injection or 4 days (*4d) after last CCl_4 treatment. Data represent mean ± SD, n = 5. (D) FACS analysis of HSCs isolated from wildtype control (naïve) or CCl_4-treated (activated) animals. Cell pools isolated from 6 livers per condition were surface stained with an antibody to CXCR3. In parallel, HSCs were

identified by intracellular GFAP staining. Numbers indicate percentage of $GFAP^+$ cells that were $CXCR3^+$.

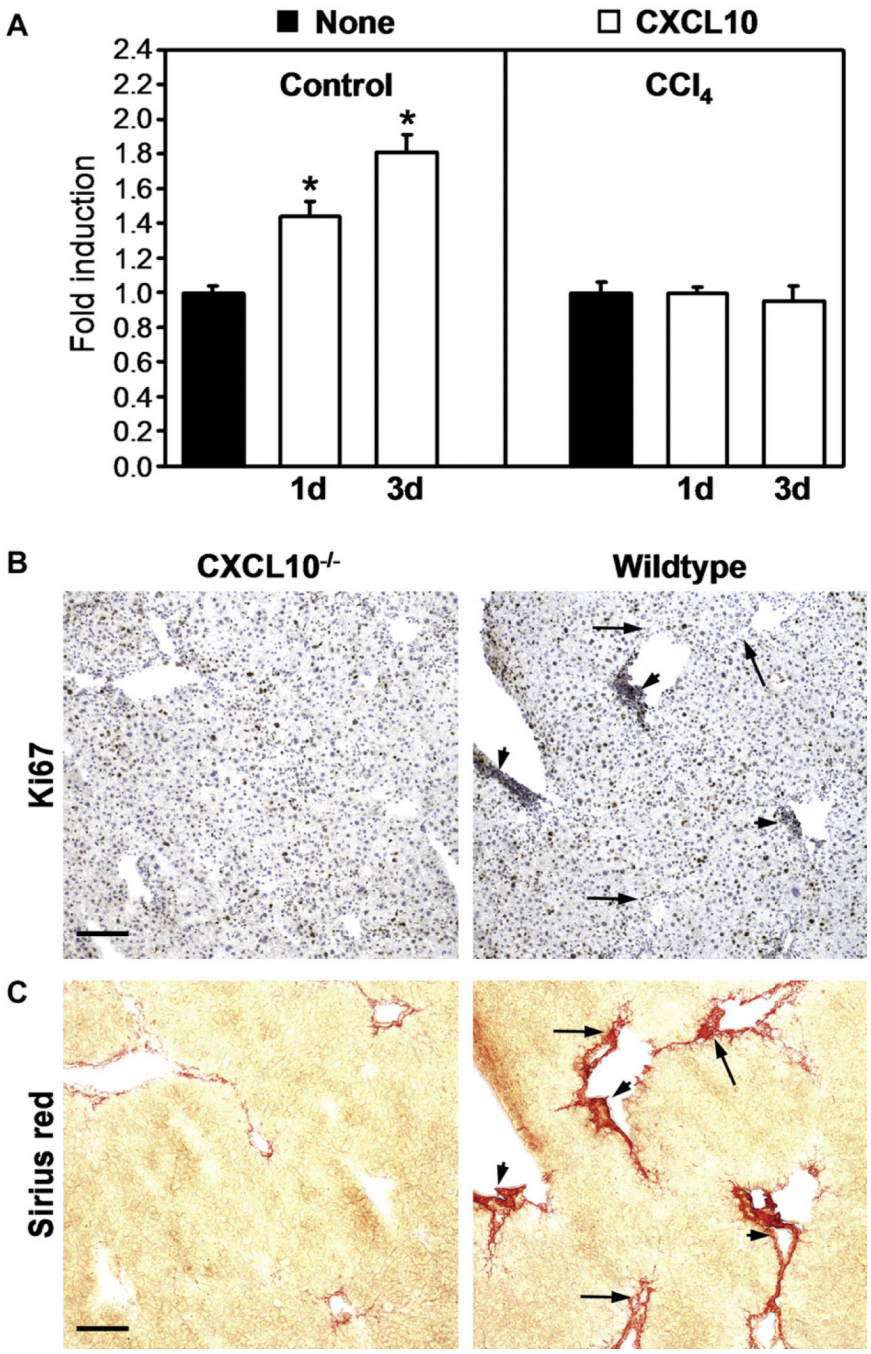

Fig. 4.

CXCL10 stimulates HSC chemotaxis but not proliferation. (A) Freshly isolated HSCs from control or CCl_4-exposed animals were seeded in Transwell chambers. Cells were stimulated with 20 ng/ml CXCL10 or were left untreated (none). Medium was renewed every day. Migration was stopped at indicated time points and cells that had migrated through the Transwell inserts were counted in 10 microscopic fields. Assays were done in duplicates and were repeated 3 times. Data are mean fold induction ± SD (n = 3) with untreated cells set at 1. *$P < 0.05$ (CXCL10 versus untreated). Consecutive liver sections of CCl_4-treated wildtype or $CXCL10^{-/-}$ mice were stained with an antibody to the proliferation marker Ki67 (B) or with Sirius Red (C). Ki67 staining was seen in hepatocytes and strongly in areas with

high numbers of infiltrating cells (arrowheads). Ki67 expression was low in regions with high fibrosis but low infiltrates (arrows). Proliferation intensity was similar in wildtype and CXCL10$^{-/-}$ livers. Scale bar = 100 μm.

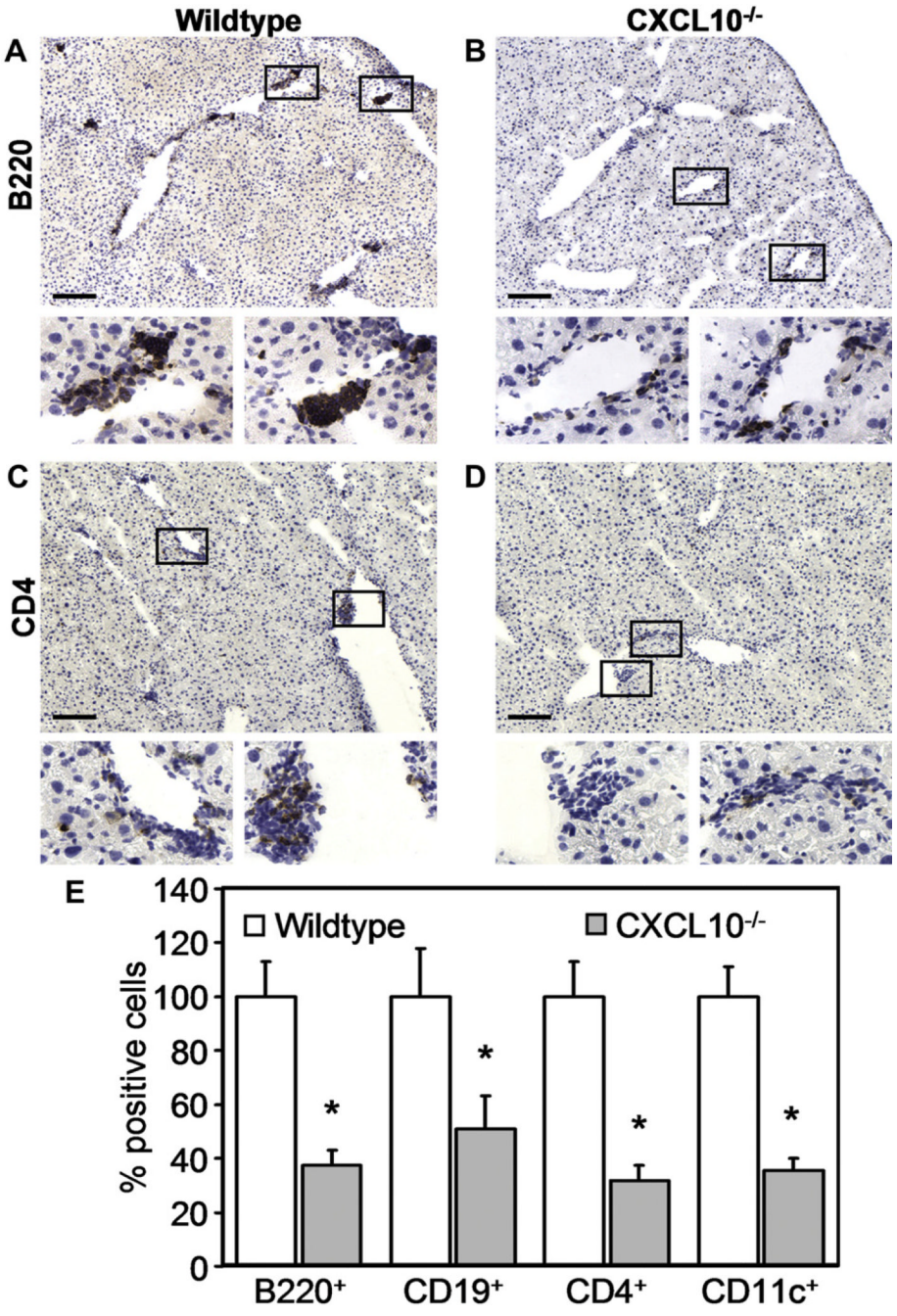

Fig. 5.

Localization of immune cells in livers of CCl_4-treated CXCL10$^{-/-}$ and wildtype mice. Mice were treated with CCl_4 for 4 weeks before livers were processed for immunohistochemistry. Tissue sections of wildtype (A and C) and CXCL10$^{-/-}$ (B and D) mice have been stained for B220$^+$ cells (A and B), CD4 T cells (C and D), CD19$^+$ cells (not shown), and CD11c$^+$ cells (not shown). Boxed areas are shown in larger magnification underneath original photomicrographs. Scale bar = 100 μm. (E) Cell numbers were counted in 10 sections of 10 different animals per group from 5 independent experiments. Relative cell numbers have been normalized to the corresponding number of B220$^+$, CD19$^+$, CD4$^+$, and CD11c$^+$ cell

infiltrations found in livers of CCl_4-treated wildtype mice. Data represent mean ± SEM. *$P < 0.05$ ($CXCL10^{-/-}$ versus wildtype).

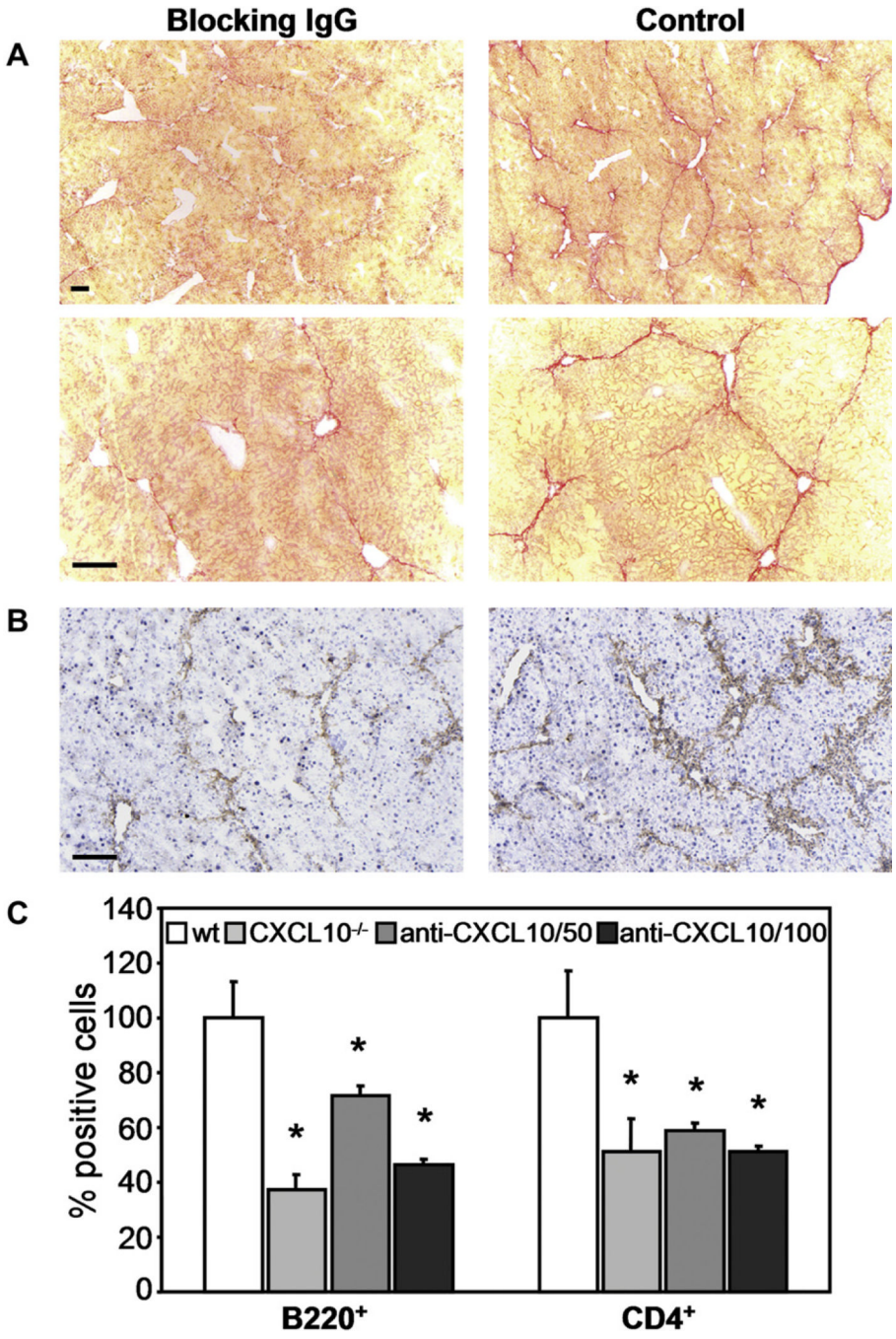

Fig. 6.

Blocking anti-CXCL10 antibody reduces liver fibrosis and number of infiltrating $B220^+$ cells and CD4 T cells. Wildtype mice were injected intraperitoneally three times per week with 50 μg or 100 μg blocking anti-CXCL10 mAb and twice a week with CCl_4. After 4 weeks, livers were collected and cryosections were stained with (A) Sirius Red (two different magnifications are shown; scale bar = 100 μm), (B) an anti-αSMA antibody or (C) antibodies to B220 or CD4 (stainings not shown). Left panels (A and B) show liver sections of mice treated with 100 μg anti-CXCL10 mAb. Control mice received 100 μg of an isotype-matched control antibody (A and B, right panel). $B220^+$ cells and CD4 T cells were counted in 10 sections of 5 different animals per group from 2 independent experiments.

Data represent mean ± SEM. *$P < 0.05$ ($CXCL10^{-/-}$ or anti-CXCL10 antibody treated versus isotype control).

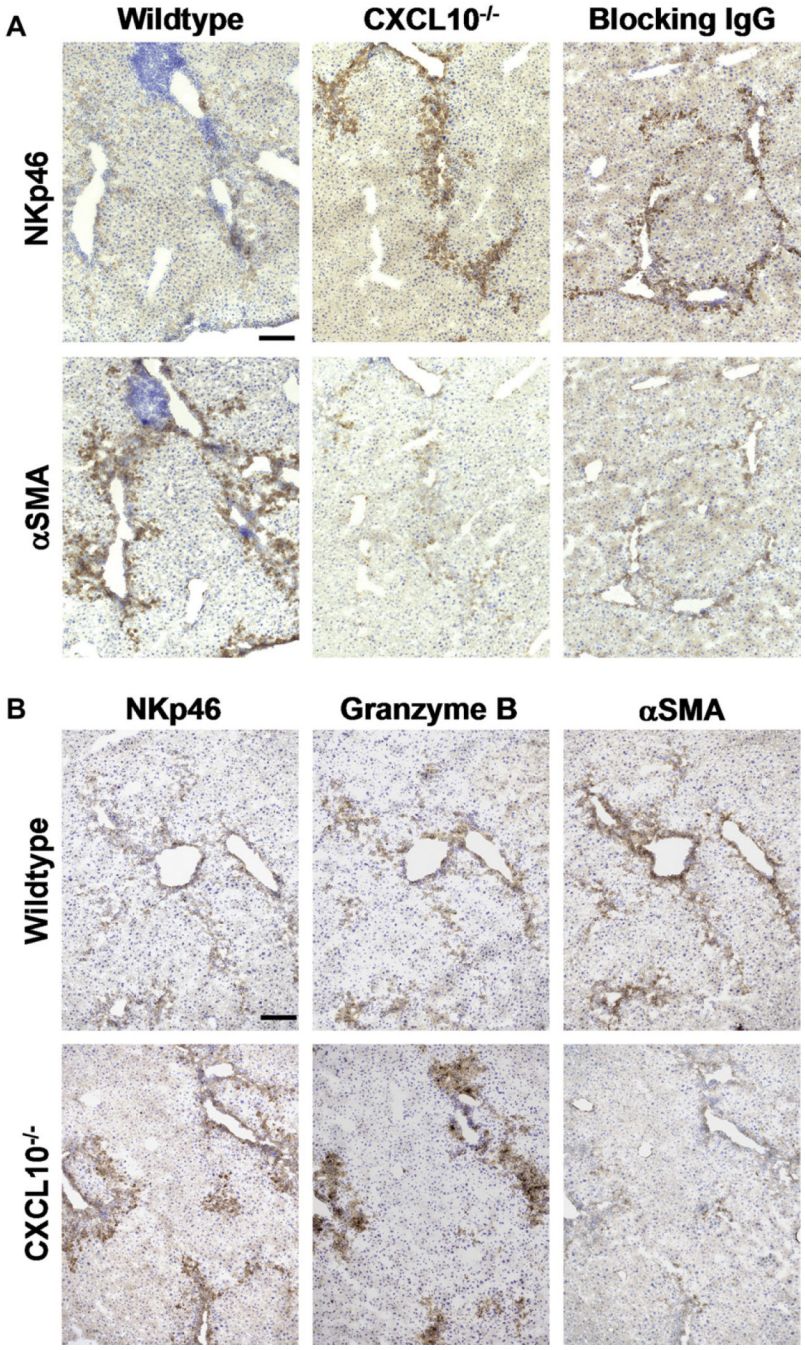

Fig. 7.

In the absence of CXCL10, increasing numbers of NK cells infiltrate the liver and eliminate activated HSCs by a granzyme B-dependent mechanism. Consecutive tissue sections from livers harvested at week 4 after start of CCl_4 administration were stained for NKp46, αSMA or granzyme B. (A) NK cell numbers were low and αSMA-expressing cells were frequent in livers obtained from wildtype mice (left panels). In contrast, the number of NK cells was 8.12 ± 1.18-fold higher and αSMA expressing cells were scarce in livers of $CXCL10^{-/-}$ mice (middle panel). Similarly, αSMA expression was low and 7.53 ± 0.94-fold more NK cells were present in mice treated with anti-CXCL10 antibody (100 μg i.p., three times per week) than in wildtype mice. Scale bar = 100 μm. Cell numbers were counted in 4 sections

of 5 different animals per group from 2 independent experiments. Relative cell numbers have been normalized to the corresponding number of $NKp46^+$ cell infiltrations found in livers of CCl_4-treated wildtype mice. Data represent mean ± SEM. $*P < 0.05$ ($CXCL10^{-/-}$ or anti-CXCL10 antibody treated versus control). (B) In wildtype livers, granzyme B staining was rather weak, correlating with the low number of NKp46-expressing cells. In contrast, αSMA-positive cells were highly abundant (upper panel). In $CXCL10^{-/-}$ livers, αSMA-expressing cells were rare, whereas the number of NK cells was high and granzyme B expression was strong (lower panels). Scale bar = 100 μm.